Accepted Manuscript

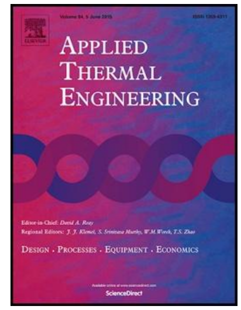

Title: Optimization of fuel injection in GDI engine using economic order quantity and lambert w function

Author: Robert Ventura, Stephen Samuel

PII:	S1359-4311(16)30157-0
DOI:	http://dx.doi.org/doi: 10.1016/j.applthermaleng.2016.02.024
Reference:	ATE 7753
To appear in:	*Applied Thermal Engineering*
Received date:	17-10-2015
Accepted date:	4-2-2016

Please cite this article as: Robert Ventura, Stephen Samuel, Optimization of fuel injection in GDI engine using economic order quantity and lambert w function, *Applied Thermal Engineering* (2016), http://dx.doi.org/doi: 10.1016/j.applthermaleng.2016.02.024.

Optimization of Fuel Injection in GDI Engine Using Economic Order Quantity and Lambert W Function

Abbreviated title: GDI Engine Control and Optimization

Robert Ventura, Stephen Samuel
Department of Mechanical Engineering and Mathematical Sciences, Oxford Brookes University, Oxford, UK

Address correspondence to Stephen Samuel, Faculty of Technology, Design & Environment, Department of Mechanical Engineering and Mathematical Sciences, Oxford Brookes University, Wheatley Campus, OX33 1HX UK.
Phone: + 44 1865 483513; email: s.samuel@brookes.ac.uk

Highlights

- EOQ approach for fuel injection event in GDI engine has been evaluated.
- Analogy between EOQ and fuel injection and combustion process has been drawn.
- Components that contribute to the loss of energy in the system have been modelled using EOQ.
- A fuel injection control strategy has been proposed using EOQ and Lambert W function.

ABSTRACT

The present work evaluated the suitability of Economic Order Quantity (EOQ), commonly used in supply chain management and process optimization, for combustion in Gasoline Direct Injected (GDI) engines. It identified appropriate sub-models to draw an analogy between the EOQ for melon picking and fuel injection in GDI engines. It used experimental data from in-cylinder combustion processes for validating the model. It used peak cylinder pressure and indicative mean effective pressure for validating the model; the R^2 value for linear correlation between the experimental value and estimated value is 0.98. This work proposes that the EOQ based on Lambert W function could be employed for optimizing the fuel quantity in GDI engines for real-world fuel economy.

KEYWORDS: *Fuel consumption, Economic Order Quantity, Lambert W function, Gasoline Direct Injection*

NOMENCLATURE

ANN	Artificial Neural Network
DISI	Direct Injection, Spark Ignition
ECU	Electronic Control Unit
EOQ	Economic Order Quantity
GDI	Gasoline Direct Injection
MVT	Marginal Value of Time
PFI	Port Fuel Injection
SMD	Sauter Mean Diameter
THC	Total hydrocarbon

1. INTRODUCTION

Improving the fuel economy of the internal combustion engines has been one of the main goals of automotive industry along with meeting emission targets set by the legislators, ever since the contribution of engine-out CO_2 from combustion engine was recognized as a contributor towards greenhouse gas inventory. The role of fuel injection and electronic control systems for increased fuel economy, reduced emission levels and overall improvement of thermodynamic efficiency of the internal combustion engines cannot be over emphasized (Heintz, et al., 2001). Therefore, it can be seen that successive legislative targets forced the vehicle manufacturers to move from carburetion to fuel injection; and within the fuel injection, from low pressure injection to high pressure injection; and crude fuel calibration procedure to various forms of complex fuel injection optimization strategy (Salazar & Ghandhi, 2006). Moving away from carburetion or port fuel injection system to direction injection system for gasoline application provides ample opportunity for metering the quantity of the fuel precisely for every cycle per cylinder in a multi-cylinder engine. In a carbureted engine, metering the quantity of fuel may not be precise; however, the time available for fuel evaporation before it reaches the cylinder or before the start of the combustion is comparatively long and therefore, the combustion takes place almost in a pre-mixed mode (Khan, et al., 2009). However, a significant proportion of unburned fuel could escape the combustion process because of the excessive wall wetting in the manifold. This excessive wall wetting increases the emission levels beyond the current requirements. Similarly, in a Port Fuel Injection system (PFI), fuel is injected in the port upstream of the intake valve; therefore, less surface area is exposed for wall wetting when compared with the carbureted system. In addition, metering the quantity of the fuel per cylinder in PFI system could be more precise when compared to carbureted engines (Zhao, et al., 1997). Similar to carbureted engines, the combustion in port injection engines also takes place in a pre-mixed mode, and therefore smoothness of the cylinder pressure leads to smooth power output. However, pre-evaporation and pre-mixing introduces another limitation on workable compression ratio for the given fuel octane rating (Zhao, et al., 1997) in addition to emission levels, even though the emission levels are significantly lower than that of carbureted engines.

In contrast to PFI engines, modern gasoline direct fuel injection engines, where the fuel is injected directly into the combustion chamber enable the designers to use higher compression ratio to improve the overall thermal efficiency of the engines. This higher compression ratio is achievable because of the charge cooling effect, which lowers the charge temperature due to the evaporation process that takes place within the combustion chamber (Singh, et al., 2014). One of the inherent limitations of this strategy is the reduced time available for the evaporation and mixing process which directly influences the mode of combustion and also emission formation mechanisms, especially nano-scale particulate matter formation in gasoline direct injection engines (Samuel, et al., 2010). Recently introduced EURO VI emission standards for light-duty vehicles includes the levels of nano-scale particulate matter from gasoline direct injection engines and therefore, it is one of the major challenges of the automotive manufacturers using GDI engines. The opportunity for operating the engine at higher compression ratio with the ability to precisely meter the fuel cycle by cycle demands a better optimization strategy in order to overcome the drawbacks of reducing injection and evaporation timing (Whelan, et al., 2012). Hence, various manufacturers are in search of complex optimization algorithms to optimize the fuel injection strategy for improved fuel economy and reduced emission levels.

One of the methods is the Genetic Algorithm. Genetic algorithms are proposed for optimizing the fuel injection strategy in gasoline direct injection engines (Tanner & Srinivasan, 2007). Artificial Neural Network (ANN) is another method that can also be applied for the optimization of the fuel injection strategy. ANN is a method commonly used for information processing based on the way biological nervous systems process information (Stergiou & Siganos, 2015) and has been applied to the air-fuel ratio control (Lenz & Schröder, 1998), characterization of DISI emissions and fuel economy (Shayler, et al., 2001) and in powertrain simulation tools (Le berr, et al., 2008). Another way of optimizing the fuel injection strategy is to identify different events and processes, which take part during fuel injection phase and use appropriate phenomenological or semi-empirical models to include the effect of those events and processes in the optimization algorithm. The submodels required for developing optimization algorithm are; fuel spray and impingement model, wall wetting and evaporation model and combustion and heat transfer models.

In GDI engines, the fuel droplets may impinge onto the combustion chamber walls because the fuel is directly injected into the combustion chamber at a higher velocity. If these fuel droplets are not completely evaporated on time they will increase the quantity of unburned fuel, and therefore THC emissions. The level of wall wetting in GDI engines is typically higher than those in port fuel injection engines due to higher injection pressures and resulting higher penetration velocity and distance (Serras-Pereira, et al., 2007). A study by Hung et al (Hung, et al., 2007) concludes that for given port flow characteristics, piston and cylinder head, injector spray pattern has higher levels of influence on the quality of air-fuel mixture. They also suggest that fuel impingement on in-cylinder walls can be minimized and fuel-air mixing could be improved by choosing an appropriate spray pattern. In the same line of argument, Mittal et al (Mittal, et al., 2010) show that split injection is an effective way to reduce the overall fuel impingement on in-cylinder surfaces.

Once the fuel spray is in the combustion chamber the amount of fuel available for combustion is determined by the rate of evaporation and the amount of fuel suspended in the air in vapour phase. This determines the quality of the fuel-air mixture (Gold, et al., 2001; Khan, et al., 2009) that in turn determines the efficiency of the combustion. The next stage is the heat transfer phase; heat lost to the wall during combustion process determines the actual amount of energy available for changing the cylinder pressure (Harigaya, et al., 1993; Hensel, et al., 2009; Morel, et al., 1988; Shayler & and May, 1995). This cylinder pressure for a given combustion chamber volume change during the overall process determine the net energy conversion from fuel to useful work output. Therefore, total quantity of the fuel injected to cylinder pressure could be used to estimate the indicated thermal efficiency of the engine. The overall thermal efficiency of the engine is only around 40% for internal combustion engines.

In the light of this brief literature review it can be concluded that identifying suitable optimization strategy for fuel injection in GDI engine is still open to research. A closer look at the phases in Economic Order Quantity (EOQ) mainly used for perishable inventory show that an analogy could be drawn by comparing the processes involved in GDI engines. This analogy is based on the fact that the injected fuel is losing its "value" as a function of time from the point of injection to "sold" in form of change in cylinder pressure. Therefore, the purpose of this study was to evaluate the suitability of the Economic Order Quantity based on Lambert W function, which has been successfully applied for perishable inventory, for fuel injection and combustion process in gasoline direction injection engine. The following section will briefly review the approach proposed by (Blackburn & Scudder, 2009) for solving Economic Order Quantity problems and show the relevant processes applicable for the present work.

2. Economic Order Quantity

Economic order quantity (EOQ) is the order quantity that minimizes the total inventory holding costs and ordering costs (Blackburn & Scudder, 2009). Blackburn and Scudder investigated the supply chain strategies for melons, a perishable and fresh product, and proposed a method for minimizing the cost value. The logical approach proposed by Blackburn and Scudder (Blackburn & Scudder, 2009) and the variables considered in their model are summarized in ***Figure 1***.

The perishable melon as a fresh product, has its peak value at the yield. After being collected, the value of the product is reduced in an exponential manner based on the time spent during different processes. The deterioration of the quality of the product has two phases; the first phase is a fast deterioration phase and then in the second phase the product is brought to the cooling facility where the deterioration is diminished. (Blackburn & Scudder, 2009). They proposed a model based on product's *marginal value of time* to minimize the lost value of the product during the supply chain. *Marginal value of time* (MVT) is defined to be the *change in value of a unit of product per unit time at a given point in the supply chain* (Blackburn & Scudder, 2009). ***Figure 2*** shows the reduction in value of the product (melons) over the time in the supply chain.

The variables in the model presented by (Blackburn & Scudder, 2009) are summarized in the flow chart ***Figure 1*** and also in ***Figure 2***. The variables corresponding to the first part of the supply chain are: total annual harvest (*D*), the transfer batch size in cartons (*Q*), maximum value of a carton of product at time t=0

(V), picking rate in cartons per hour (P), deterioration rate in value of product per hour (α), batch transfer time in dollars (K) and transfer time in hours from field to the cooling facility (t_r).

The variables that were selected during the second part of the supply chain corresponding to the time when the product is in the cooling facility are: deterioration in value of product per time (β), time (t_j) and the cost of the transportation to the retailer (C_j).

The cost equation proposed by (Blackburn & Scudder, 2009) using these variables was:

$$TC = \frac{K \cdot D}{Q} + D \cdot V - \frac{D}{Q \cdot \alpha} \cdot \left(p \cdot V \cdot e^{-\beta \cdot t_j} \cdot e^{-\alpha \cdot t_r}\right) \cdot \left(1 - e^{-Q \cdot \alpha / p}\right) + c \cdot D + C_j \qquad (1)$$

And the minimum cost equation ignoring the variables D and C_j was:

$$minTC = \frac{1}{Q}\left[K - \left(p \cdot e^{-\beta \cdot t_j} \cdot e^{-\alpha \cdot t_r} \cdot V / \alpha\right) \cdot \left(1 - e^{-Q \cdot \alpha / p}\right)\right] \qquad (2)$$

(Blackburn & Scudder, 2009) Also proposed that the optimal Q in the form of Lambert W function satisfies:

$$Q = \left(\frac{p}{\alpha} - k\right) \cdot e^{Q \cdot \alpha / p} - \frac{p}{\alpha} \qquad (3)$$

Where the constant k corresponds to:

$$k = e^{\alpha \cdot t_r + \beta \cdot t_j} \,.\, K / V \qquad (4)$$

2.1 Analogy EOQ with fuel injection event

A closer look at the phases in EOQ and the process involved in GDI combustion show that an analogy could be drawn. This analogy is based on the fact that the injected fuel is losing its "value" as a function of time from the point of injection to "sold" in form of change in cylinder pressure.

The first part of deterioration is considered to be the fuel that remains in the piston after the wall wetting event. For this first part, evaporation during injection and wall wetting models have been developed. This part is comparable to the phase where the melon is picked from the vine until it is brought to the cooling facility in the melon supply chain. Second part of deterioration phase in the cooling facility is comparable the heat transfer and energy loss in the combustion chamber. The final output from this analogy is the quantity of fuel to be injected in order to optimize the peak pressure and the mean effective pressure values. ***Figure 3*** shows the analogy between economic order quantity and the fuel injection event observed using the reduction of the product value over the time.

3. Lambert W function in EOQ

The Lambert W function, W[z], is the inverse function of $z = w[z]e^{w[z]}$ (Corless, et al., 1996), where "e" is the natural exponential number and "z" a complex number. The real part of the solution to the Lambert W function in terms of x is shown in ***Figure* 4**.

The Lambert W function does not differ too much from the inverse trigonometric functions. This function is a multi-valued function on a given domain, and a *principal branch* needs to be defined. When "x" is real, as can be seen in ***Figure* 4**, it has two solutions in the interval -1/e < x < 0. The branch that satisfies W[z] ≥-1 is named W_0[z], and is defined to be the principal branch (solid line in ***Figure* 4**) , while the secondary real branch that satisfies W[z] ≤ -1 is designated W_{-1}[z] (dashed line in ***Figure* 4**) (Stewart, 2005). Recently, Disney and Warburton (Warburton, 2009; Disney & Warburton, 2012) introduced Lambert W function for solving EOQ problems successfully. Following Disney & Warburton's study (Disney & Warburton, 2012), Lambert W function has been found to be very useful for the EOQ problems with perishable inventory by improving their lower bound for the optimum order quantity. Therefore, Lambert W function is used in this study in order to determine the optimum fuel quantity based on the scheme used for Melon picking by (Disney & Warburton, 2012).

Rearranging ***equation 3*** (Disney & Warburton, 2012):

$$\frac{p}{\alpha} - k = \left(Q + \frac{p}{\alpha}\right) \cdot e^{-\alpha Q/p} \quad \textbf{(5)}$$

$$\frac{\alpha k}{pe} - \frac{1}{e} = \left(-\frac{Q\alpha}{p} - 1\right) \cdot e^{\left(-\frac{Q\alpha}{p} - 1\right)} \quad \textbf{(6)}$$

The ***equation 6*** is in the form of Lambert W function ($y = xe^{x}$), and the solution can be obtained by $x = W[y]$. Therefore, the exact solution is found in the W_{-1} branch of Lambert W function as follows.

$$-\frac{Q\alpha}{p} - 1 = W_{-1}\left[\frac{\alpha k}{pe} - \frac{1}{e}\right] \quad \textbf{(7)}$$

$$Q^{*} = -\frac{p}{\alpha}\left(W_{-1}\left[\frac{\alpha k}{pe} - \frac{1}{e}\right] + 1\right) \quad \textbf{(8)}$$

The optimal value implies that Q^{*} does not exist if one of the values of $\{p, k, \alpha\}$ is negative, or if an even (or zero) number of $\{p, k, \alpha\}$ are negative and $V < (\frac{e^{\alpha \cdot t_r + \beta \cdot t_j} K\alpha}{p})$ (Disney & Warburton, 2012). Notice that in the equation of the optimal value for Q^{*} a branch of Lambert W function is defined since the optimal order quantity, the deterioration rate, and the picking rate are always positive. Therefore follows $W[z] < -1$, which only happens on $W_{-1}[z]$, the secondary branch.

4. Fuel injection and combustion model based on EOQ

The possibility of developing an analogy between EOQ and fuel injection and combustion process in GDI engines is clear by drawing parallels between the EOQ and the physical process involved in fuel injection and combustion in GDI engines. In order to employ and validate this analogy, the details relating to appropriate mathematical models that could be used to represent the physical processes such as fuel injection and spray model, wall wetting and evaporation and heat transfer are essential and therefore, the following sections provide the details of these models from the published literature.

4.1 Fuel Spray model

Direct injection engines have the injectors mounted in the cylinder head and the fuel is injected directly into the combustion chamber. As fuel is added during the compression stroke, only a short period is available for the completion of evaporation and mixing process (Pulkrabek, 2003). Fuel injectors in direct injected engines must operate with relatively high injection pressure when compared to port fuel injected engines. A fuel spray model that includes vaporization process should be capable of predicting the occurrence of wall-wetting in order to estimate the amount of fuel available for combustion. This work employs Hiroyasu model since this model is known to give very good correlations with the experimental data (Boot, et al., 2007). Hiroyasu model (Hiroyasu, et al., 1993) considers mass of the fuel quantity evaporated during injection and the spray tip penetration, to quantify the mass of fuel that will hit the piston. The fuel mass evaporated will mix with the air and, therefore, is available for combustion. The remaining quantity of fuel (hitting the piston) is estimated using a suitable wall-wetting model for evaluating the final quantity of fuel available for combustion. Hiroyasu model divides the spray into multiple radial and axial packages as shown in ***Figure 5***. This model assumes no interaction between the packages; it considers that each package initially consists of droplets of one unique diameter and the ambient gas entrainment is controlled by conservation of momentum only.

Based on (Boot, et al., 2007) these information, two main phases can be identified in the spray development. The first phase is named as pre-breakup area, where the jet travels freely at a constant velocity. Spray tip penetration in the pre-breakup area could be estimated using Bernoulli's equation as shown below:

$$x(t) = C_a \cdot C_v \sqrt{\frac{2 \cdot (p_{inj} - p_a)}{\rho_f}} \cdot t = C_d \sqrt{\frac{2 \cdot (p_{inj} - p_a)}{\rho_f}} \cdot t \tag{9}$$

The coefficients C_a and C_v are measures for losses in the orifice area and velocity due to cavitation and frictional effects respectively. The introduction of the discharge coefficient is not part of the Hiroyasu model, but it was proposed to account for the dissimilarities in injector orifice dimensions between modern and older designs (Boot, et al., 2007). In this study the discharge coefficient is fixed to 0.39 and p_{inj} corresponds to the injection pressure, p_a to the pressure in the combustion chamber at the start of injection point obtained from the experimental in-cylinder pressure data acquired and ρ_f is the fuel density.

Atomization due to ambient gas entrainment is assumed to occur after a certain break-up time:

$$t_{b,k} = 4.351 \cdot \frac{\rho_f \cdot d}{{C_d}^2 \sqrt{\rho_a \cdot (p_{inj} - p_a)}} \cdot \left(\frac{6-k}{5}\right) \tag{10}$$

Where k is the radial index based on the assumption that the initial jet periphery is more exposed to the ambient gas than the core, ρ_a corresponds to the in-cylinder air density, and d is the injector orifice dimension. As assumed by Boot et al. (Boot, et al., 2007) only the tip penetration along the central axis (*k=1*) is considered since at this location wall wetting is most prevalent. Therefore, the model is assumed to be a 1D model.

In a given radial package *k* at $t = t_{b,k}$, the Sauter Mean Diameter (SMD) (Boot, et al., 2007) is:

$$SMD = d \cdot max\left[\frac{SMD^{LS}}{d}, \frac{SMD^{HS}}{d}\right] \tag{11}$$

$$\frac{SMD^{LS}}{d} = 4.12 \cdot Re^{0.12} \cdot We^{-0.75} \cdot \left(\frac{\mu_f}{\mu_a}\right)^{0.54} \cdot \left(\frac{\rho_f}{\rho_a}\right)^{0.18} \tag{12}$$

$$\frac{SMD^{HS}}{d} = 0.38 \cdot Re^{0.25} \cdot We^{-0.32} \cdot \left(\frac{\mu_f}{\mu_a}\right)^{0.37} \cdot \left(\frac{\rho_f}{\rho_a}\right)^{-0.47} \tag{13}$$

Initial diameter of the liquid fuel droplets right after the breakup time in each zone can be calculated using ***equations 11-13*** and assuming normal distribution. Hence, the number of droplets in each zone can be calculated knowing the SMD and the mass of fuel injected (Jung & Assanis, 2001). Where μ_a and μ_f are the dynamic viscosity of gas in the cylinder and the dynamic viscosity of the fuel respectively, and Re is the Reynolds number.

We is the Weber number, which is a dimensionless quantity for analysing the interface between two fluids and is defined as follows:

$$We = \frac{[\rho_a \cdot v^2 \cdot D]}{\sigma} \tag{14}$$

Where v is the droplet normal impact velocity estimated using the fuel mass rate, D is the characteristic length, in this case the droplet diameter and σ is the fuel surface tension for octane.

Similarly, penetration in the post-breakup area will occur when the ambient gas is entrained into a spray packet, at this point its velocity will decrease and the penetration at this stage could be estimated as follows (Boot, et al., 2007):

$$x(t)_{k=1} = 2.95 \cdot \left(\frac{p_{inj} - p_a}{\rho_a}\right)^{1/4} \sqrt{d \cdot (t - t_{b,k})} + C_d \sqrt{\frac{2 \cdot (p_{inj} - p_a)}{\rho_f}} \cdot t_{b,k} \tag{15}$$

A simplified droplet evaporation model as applied by (Boot, et al., 2007) based on (Lefebvre, 1989) was chosen for this study as follows:

$$\frac{dD}{dt} = \frac{4 \cdot k_a \cdot \ln(1 + B_m)}{\rho_f \cdot c_{p,a} \cdot D} \quad \textbf{(16)}$$

$$\frac{dm_D}{dt} = 2\pi \cdot D \cdot \frac{k_a}{c_{p,a}} \cdot \ln(1 + B_m) \quad \textbf{(17)}$$

$$\frac{dT_{f,s}}{dt} = \frac{dm_D}{dt} \cdot \frac{L_{f,s}}{c_{p,f,s} \cdot m_D} \cdot \left(\frac{B_T}{B_M} - 1\right) \quad \textbf{(18)}$$

The subscripts *a*, *f* and *s* correspond to the conditions in the ambient gas, liquid fuel and on the droplet surface temperature and the variables k, c_p , L_s , B_T and B_M correspond to thermal conductivity, specific heat, latent heat of evaporation and the heat and mass transfer numbers respectively.

4.2 Wall Wetting Model

The fuel droplets may impact onto the combustion chamber walls due to the fuel directly being injected at a high speed in GDI engines and this impingement on walls will affect the performance of the engine. If these fuel droplets are not evaporated completely before the start of combustion they will increase unburned fuel mass, and therefore increase the levels of THC and soot emission levels.

The evaporation process in this study is modelled using the method proposed by Curtis et al. (Curtis, et al., 1996). Although the model described by (Curtis, et al., 1996) is developed for a port fuel injected engine, the cylinder wall wetting model part can be implemented in the gasoline direct injection engine of this study considering only one film. The predictions for in-cylinder liquid fuel mass made by (Curtis, et al., 1996) were found to give reasonable prediction, hence a good correlation between the complexity of the model and the output given by the model is found using this method. The equation presented for the mass vaporization rate is:

$$\dot{m}_v = Sh\left(\frac{A_{ls}}{B}\rho_{gm}D_{fa}\ln\left(1 + \frac{\Delta MFF}{(1 - MFFs)}\right)\right) \quad \textbf{(19)}$$

Where A_{ls} corresponds to the liquid surface area, ρ_{gm} is fuel density, D_{fa} Corresponds to the mass diffusion coefficient between the fuel and the air, ΔMFF Stands for the difference in mass fraction of fuel in the vapour at the liquid surface and the free stream, $MFFs$ is the mass fraction of fuel in the vapour at the liquid surface, Sh is the Sherwood number, which is calculated by:

$$Sh = (1 + 0.023Re^{0.83}Sc^{0.33}) \quad \textbf{(20)}$$

4.3 Heat Transfer Model

One of the most important parameters related with engine performance, fuel economy and emission levels is the thermal efficiency. The most significant operating variable which is directly linked to thermal efficiency which can be controlled is heat loss from the combustion and expansion stroke (Andrews, et al., 1989). GDI engines suffer significantly during cold start because of the poor evaporation of the fuel and the air-fuel ratio fluctuation due to wall wetting (Lahuerta & Samuel, 2013). This work uses Woschni's heat transfer model (Woschni, 1967) for estimating heat transfer rate in the combustion chamber during compression, gas exchange, combustion and expansion process separately. This study assumes steady state considering that the role of convection is predominant compared with radiation (Hensel, et al., 2009) in gasoline engines inside the combustion chamber. The heat transfer between the air-fuel mixture and the gas side of the cylinder wall is calculated using the Newton's Law of convection:

$$Q = h_c \cdot A \cdot (T_g - T_w) \quad \textbf{(21)}$$

Where h_c corresponds to the convection coefficient which depends on the Nusselt, Reynolds and Prandtl numbers. *A* is the exposed area where the heat transfer is present, T_g is the mean gas temperature and T_w is the wall temperature.

The convection coefficient can be obtained by using the Woschni's heat transfer model, assuming a correlation based on Reynolds and Nusselt number, the convection coefficient is:

$$h_c = C \cdot B^{m-1} \cdot p^m \cdot w^m \cdot T^{0.75-1.62} \quad \textbf{(22)}$$

Where *C* and *m* are empirical coefficients which take the values 0.0035 and 0.8 (Woschni, 1967) and *P* is the pressure and *T* is the temperature of the gas inside the combustion chamber. The average gas velocity *w* is determined by considering four-stroke, water-cooled and direct injection without swirl motion (Heywood, 1988):

$$w = C_1 \cdot \bar{S}_p + C_2 \cdot \frac{V_d \cdot T_r}{p_r \cdot V_r} \cdot (p - p_m) \quad \textbf{(23)}$$

Where V_d is the displacement volume, p_r, V_r and T_r are the fluid pressure, volume and temperature at a reference state, and p_m is the isentropic pressure. Coefficients C_1 and C_2 depend on the phase of the engine cycle, for combustion and expansion are 2.28 and $3.24 \cdot 10^{-3}$ respectively (Nieuwstadt, et al., 2000).Once the convection coefficient is known, heat losses can be estimated using the Newton's Law of convection (*equation 21*). It is important to note that, with the aim of achieving a good relation between complexity of the model and the output given, heat transfer losses have been calculated by using in-cylinder mean gas temperature, mean wall temperature and pressure at the start of combustion.

4.4 Fuel Injection Optimization Using Lambert W function based on EOQ

The analogy between variables is shown in ***Table 1***. Although the analogy is based on the fact that the injected fuel is losing its "value" as a function of time from the point of injection to "sold" in form of change in cylinder pressure, each variable in EOQ could be mapped against corresponding variable in the fuel injection and associated process in the combustion chamber.

Once the mapping of the relationship between the economic order quantity variables and the fuel injection event variables is done, the solution for the optimal fuel injection quantity can be found. Now, the optimal quantity of fuel mass can be estimated as shown in ***equation 24***. The decision variable for the fuel injection problem is assumed to be the difference between the original injected fuel mass and the optimal fuel mass to be injected.

$$Q^* = -\frac{p}{\alpha}\left(W_{-1}\left[\frac{\alpha k}{pe} - \frac{1}{e}\right] + 1\right) * InjectionDuration \quad \textbf{(24)}$$

The data required for applying the optimization equation are obtained using the wall wetting, evaporation and heat transfer models. Once all data is obtained, the equation is solved and the fuel mass quantity to subtract from the original value is known. Therefore, the total quantity of fuel to be injected is estimated and the required new injection time is obtained. It is important to note that the main output from that model is the new injection duration, as the fuel mass flow rate is imposed by the injector, injection pressure and combustion chamber conditions. The present work used MATLAB® for solving wall wetting, evaporation and heat transfer models and for analytical solving Lambert W function.

5. Results and discussion

5.1 Engine

A Euro-IV compliant, 1.6-L, four-cylinder in-line, GDI, turbocharged and intercooled spark ignition engine was used in this study. The specifications of the engine are listed in ***Table 2***:

Experiments have been carried out at 3 different speeds (2000, 2400 and 2800 rpm) and at different loading conditions at each operating speed (20, 40, 60. 80, 100 and 120 Nm).

5.2 Model validation

In order to validate the heat transfer and wall wetting models, measured in-cylinder pressure was used. The results are validated using peak cylinder pressure and area under the curve. Since the peak pressure has direct correlation with the location of maximum heat release and the area under the curve represents the indicative work, i.e., cumulative energy release, these two variables were chosen for validation. The selected area is in the range from -30 crankshaft angle to +70 crankshaft angle which includes latest part of compression, duration where the impact of evaporation on cylinder pressure is dominant, combustion and early part of expansion. The results of peak pressure and area under the pressure curve after applying the fuel spray model, the wall wetting model and heat transfer model and carrying out the model validation are summarized in the Annex A.

Estimated peak pressure values (for model validation purpose) versus experimental peak pressure values for the engines conditions are shown in ***Figure 6a***. Similarly ***Figure 6b*** shows the area under the curve.

Experimental value and the estimated values show linear correlations and the R^2 value is 0.98 for the peak pressure as well as for the indicated mean effective pressure. It shows acceptable level of correlations for validation purposes.

5.3 Fuel injection optimization using Lambert W function results

The results obtained regarding the quantity of fuel to be injected are summarized in Figure 8**:**

For the given operating conditions, the possibility of using EOQ for optimizing the fuel quantity was studied. As can be observed in ***Table 3*** and **Figure *7***, at each engine condition fuel was optimized using Lambert W function based on Economic Order Quantity. As previously mentioned, the main output from the model is the new injection duration for a given fuel pressure and flow rate through the injector, as the fuel mass flow rate is imposed by the injector, injection pressure and combustion chamber conditions. Therefore, the final values of injection duration is summarized in the following table:

The main difference between the original mode of operation and the mode resulting from the optimization is the change of air fuel ratio. After applying the analogy between EOQ and fuel injection process, different amount of fuel is injected for the same air mass in the cylinder, hence the air fuel ratio needs to be controlled if a fixed-air fuel ratio is maintained at a constant value. The final air-fuel ratio obtained for each engine condition can be observed in Table 4. However, if employed, air-fuel ratio could be adjusted using air-flow controls

5.4 Control Strategy

The implementation of this method in the Electronic Control Unit (ECU) could be done by adding a new stage in the electronic control unit after the initial calculation of the ECU based on fuel pressure, fuel temperature and air mass flow rate, the injection duration is set to meet a total fuel mass quantity to be injected. Lambert W function based on economic order quantity could be used for determining the optimized mass of fuel to be injected for the for the real-world fuel economy once the base map is generated.

One of the main limitations of this study is that the current study used the experimental data to develop and verify the model, however, we couldn't deploy the model through ECU to study the effectiveness of the model since the purpose of the study is to identify the possibility of using EOQ for fuel injection strategy. The application of EOQ using Lambert W function offers promising direction because of the properties of Lambert W functions.

The final output is the new injection time that allows the ECU to inject the optimum quantity of fuel.

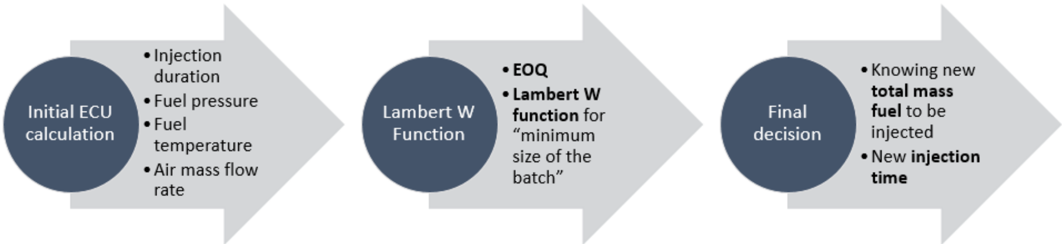

6. Conclusions

This work investigated the application of the Economic Order Quantity problem with perishable product to optimize the quantity of fuel to be injected in GDI engine through the use of Lambert W function.

1. Evaporation, wall wetting and heat transfer models have been developed in order to see how it affects the fuel consumption. These models have been validated with two in-cylinder pressure based validation models based on peak pressure and area under the pressure curve. The models have been considered suitable for representing the events of fuel spray, wall wetting and heat transfer during engine operation.
2. Analogy between Economic Order Quantity and fuel injection has been successfully established. It has been demonstrated that the exponential deterioration of the product can be applied to the in-cylinder fuel events from injection until peak pressure.
3. By applying Lambert W function to the analogy between EOQ and fuel injection, the quantity of fuel to be injected can be optimized, and consequently the injection duration. The present study shows that for the current experimental engine an average fuel saving of 5.71% could be achieved for the engine conditions studied.

REFERENCES

Jung, D. & Assanis, D. N., 2001. Multi-Zone DI Diesel Spray Combustion Model for Cycle Simulation Studies of Engine Performance and Emissions. *SAE Technical Paper Series,* Issue 2001-01-1246.

Andrews, G., Harris, J. & Ounzain, A., 1989. Transient Heating and Emissions of an SI engine During the Warm-up Period. *SAE Paper,* Volume 880264.

Blackburn, J. & Scudder, G., 2009. Supply Chain Strategies for Perishable Products: The Case of Fresh Produce. *Prod. Oper. Manag. (2),* pp. 127-137.

Boot, M. et al., 2007. On the Behavior of Fuel Spray Models in a HCCI Environment. *Proceedings of the European Combustion Meeting 2007,* pp. 1-6.

Cheng, Y.-C. & Hwang, C., 2006. Use of the Lambert W function for time-domain analysis of feedback fractional delay systems. *IEE Proc. -Control Theory Appl.,* Issue 2, p. 153.

Coreless, R., Jeffrey, D. & Valluri, S., 2000. Some applications of the Lambert W function to physics. *Can. J. Phys.,* Volume 78, pp. 823-831.

Corless, R. et al., 1996. On the Lambert W function. *Adv. Comput. Math,* Volume 5, pp. 329-359.

Curtis, E. W., Aquino, Charles F, Trumpy, David K & Davis, George C, 1996. A New Port and Cylinder Wall Wetting Model to Predict Transient Air / Fuel Excursions in a Port Fuel Injected Engine. *SAE Technical Paper,* Issue 961186.

Cwikowski, P. & Teodorczyk, A., 2009. The latest achievements in gasoline and diesel injection technology for the internal combustion engines. *Journal of KONES Powertrain and Transport,* 16(2).

D. A., 2015. *delphi.com.* [Online]
Available at: http://delphi.com/manufacturers/auto/powertrain/gas/injsys/homogenous
[Accessed 24 07 2015].

Dence, T. P., 2013. A Brief Look into the Lambert W Function. *Applied Mathematics,* Volume 4, pp. 887-892.

Disney, S. M. & Warburton, R. D., 2012. On the Lambert W function: Economic Order Quantity applications and pedagogical considerations. *Int. J. Production Economics,* 140(2), pp. 756-764.

Gäfvert, M., Arzén, K., Bernhardsson, B. & Pedersen, L., 2003. Control of Gasoline DIrect Injection using Torque Feedback: A simulation study. *Nonlinear and Hybrid System in Automotive COntrol,* pp. 289-319.

Gold, M., Stokes, J. & Morgan, R., 2001. *Air-Fuel Mixing in a Homogeneous Charge DI Gasoline Engine.* s.l., SAE.

Harigaya, Y., Toda, F. & and Suzuki, M., 1993. *Local Heat Transfer on a Combusion Chamber Wall of a Spark Ignition Engine.* s.l., SAE.

Heintz, N. et al., 2001. An approach to torque-based engine management systems. *SAE Papers,* Issue 2001-01-0269.

Hensel, S. et al., 2009. Investigations on the Heat Transfer in HCCI Gasoline Engines. *SAE Papers,* Issue 2009-01-1804.

Heywood, J., 1988. *Internal Combustion Engine Fundamentals.* ISBN:978-0070286375 ed. New York: McGraw-Hill.

Hiroyasu, H., Yoshizaki, T. & Nishida, K., 1993. Approach to Low NOx and Smoke Emission ENgines by Using Phenomenological Simulation. *SAE Paper,* Volume 930612.

Hung, D. L. S. et al., 2007. A High Speed Flow Visualization Study of Fuel Spray Pattern Effect on Mixture Formation in a Low Pressure Direct Injection Gasoline. *SAE Technical Paper,* 2007-01-14(724).

Jones, S., Shayler, P., Horn, G. & Eade, D., 2001. Engine Spark and Fuel Injection Timings. Effects, Compromise and Robustness. *SAE Paper,* Issue 2001-01-3672.

Khan, M., Watson, H. & Baker, P., 2009. Mixture Preparation Effects on Gaseous Fuel Combustion in SI Engines. *SAE Papers,* Issue 2009-01-0323.

Lahuerta, J. & Samuel, S., 2013. Numerical Simulation of Warm-Up Characteristics and Thermal Management of a GDI Engine. *SAE Paper,* Volume 2013-01-0870.

Le berr, F. et al., 2008. Powertrain Simulation Tools and Application to the Development of a SI Engine Concept Car. *SAE Paper,* Issue 2008-01-0356.

Lefebvre, A., 1989. *Atomization and Sprays.* New York: Hemisphere.

Lenz, U. & Schröder, D., 1998. Air-Fuel ratio Control for Direct Injecting Combustion Engines Using Neural Networks. *SAE Papers,* Issue 981060.

Marriott, C. D., Wiles, M. A. & Rouse, B. T., 2009. Development, Implementation, and Validation of a Fuel Impingement Model for Direct Injected Fuels with High Enthalpy of Vaporization. *SAE Papers,* Issue 2009-01-0306.

Mittal, M., Hung, David L S, Zhu, Guoming & Schock, Harold, 2010. A Study of Fuel Impingement Analysis on In- Cylinder Surfaces in a Direct-Injection Spark- Ignition Engine with Gasoline and Ethanol-Gasoline Blended Fuels. *SAE Technical Paper,* Volume 2010-01-21.

Morel, T., Rackmil, C., Keribar, R. & and Jennings, M., 1988. *Model for Heat Transfer and Combustion in Spark Ignition Engines and its comparison with Experiments.* s.l., SAE.

Muñoz, R. H., Han, Z., VanDerWege, B. A. & Yi, J., 2005. Effect of Compression Ratio on Stratified-Charge Direct-Injection Gasoline Combustion. *SAE Papers,* Issue 2005-01-0100.

Nieuwstadt, M. J. V., Kolmanovsky, I V, Brehob, D & Haghgooie, M, 2000. Heat Release Regressions for GDI Engines. *SAE Paper,* Volume 2000-01-0956.

P. B. Brito, F. Fabiao & A. Staybyn, 2008. Euler, Lambert, and the Lambert W Function today. *Applied Probability Trust.*

Pulkrabek, W. W., 2003. *Engineering Fundamentals of the Internal Combustion Engine (2nd Edition).* 2nd edition ed. University of Wisconsin - Platteville: Prentice Hall.

Salazar, V. & Ghandhi, J., 2006. *Liquid Fuel Effects on the Unburned Hydrocarbon Emissions of a Small Engine.* s.l., s.n.

Samuel, S., Hassaneen, A. & Morrey, D., 2010. Particulate Matter Emissions and the Role of Catalytic Converter During Cold Start of GDI Engine. *SAE Papers,* Issue 2010-01-2122.

Serras-Pereira, J., Aleiferis, P., Richardson, D. & Wallace, S., 2007. Spray Development in a Direct-Injection Spark-Ignition Engine. *SAE Paper,* Issue 2007-01-27.

Shayler, P. & and May, S., 1995. *Heat Transfer to the Combustion Chamber walls in Spark Ignition Engines.* s.l., SAE.

Shayler, P., Jones, S., Horn, G. & Eade, D., 2001. Characterisation of DISI Emissions and Fuel Economy in Homogeneous and Stratified Charge Modes of Operation. *SAE Paper,* Issue 2001-01-3671.

Singh, A., Lanjewar, A. & Rehman, A., 2014. Direct Fuel Injection System in Gasoline Engine. *IJITEE,* Issue 4, pp. 21-28.

Stergiou, C. & Siganos, D., 2015. *doc.ic.ac.uk.* [Online]
Available at: http://www.doc.ic.ac.uk/~nd/surprise_96/journal/vol4/cs11/report.html#What is a Neural Network
[Accessed 24 07 2015].

Stewart, S., 2005. Exact answers, old problems, and a new elementary function. *Pet. Institute, United Arab Emirates.*

Tanner, F. X. & Srinivasan, S., 2007. Global Optimization of a Two-Pulse Fuel Injection Strategy for a Diesel Engine Using Interpolation and a Gradient-Based Method. *SAE Paper,* Issue 2007-01-0248.

Warburton, R., 2009. EOQ extensions exploiting the Lambert W function. *Eur. J. Ind. Eng.,* pp. 45-96.

Whelan, I., Smith, W., Timoney, D. & Samuel, S., 2012. The Effect of Engine Operating Conditions on Engine-out Particulate Matter from Gasoline Direct-injection Engine during Cold-start. *Sae Papers,* Issue 2012-01-1711.

Woschni, G., 1967. A Universally Applicable Equation for the Instantaneous Heat Transfer Coefficient in the Internal Combustion Engine. *SAE Paper,* Volume 670931.

Zhao, F., Lai, M. & Harrington, D., 1997. *A Review of Mixture Preparation and Combustion Control Strategies for Direct-Injection Gasoline Engines.* s.l., s.n.

ANNEX A

Evaporation, Wall Wetting and Heat Transfer validation results

Peak pressure results:

	Load (Nm)	Theoretical Peak pressure (bar)	Experimental peak pressure (bar)	% Difference
2000 rpm	20	18.26	17.25	+ 5.53
	40	25.27	24.97	+ 1.19
	60	34.99	32.11	+ 8.22
	80	42.33	39.43	+ 6.85
	100	52.80	47.48	+ 10.08
	120	58.76	54.44	+ 7.36
2400 rpm	40	16.14	13.72	+ 14.98
	60	19.10	19.78	- 3.57
	80	28.70	28.21	+ 1.70
	100	39.93	37.84	+ 5.24
	120	50.39	46.33	+ 8.04
2800 rpm	40	16.71	19.96	- 19.48
	60	24.18	23.57	+ 2.50
	80	29.70	31.26	- 5.25
	100	43.11	39.08	+ 9.37
	120	53.75	48.12	+ 10.48

Area under the pressure curve results:

	Load (Nm)	Theoretical area (bar*deg)	Experimental area (bar*deg)	% Difference
2000 rpm	20	1298.10	1220.30	+ 5.99
	40	1816.80	1750.34	+ 3.66
	60	2436.42	2261.20	+ 7.19
	80	2933.74	2786.74	+ 5.01
	100	3582.02	3316.47	+ 7.41
	120	3961.90	3787.70	+ 4.40
2400 rpm	40	1134.22	1010.60	+ 10.90
	60	1423.89	1447.88	- 1.68
	80	2054.67	2029.10	+ 1.25
	100	2707.52	2670.53	+ 1.37
	120	3337.79	3238.00	+ 2.99
2800 rpm	40	1258.49	1434.97	- 13.94
	60	1702.46	1682.46	+ 1.17
	80	2122.54	2212.54	- 4.24
	100	2950.59	2754.27	+ 6.65

	120	3645.75	3371.55	+ 7.52

Fuel injection optimization using Lambert W function Results

Peak pressure results:

	Load (Nm)	Experimental peak pressure (bar)	Peak pressure after Lambert W function (bar)	% Difference
2000 rpm	20	17.25	17.53	+ 1.61
	40	24.97	24.13	- 3.47
	60	32.11	33.32	+ 3.64
	80	39.43	39.67	+ 0.62
	100	47.48	49.41	+ 3.90
	120	54.44	54.72	+ 0.51
2400 rpm	40	13.72	15.43	+ 11.07
	60	19.78	18.17	- 8.85
	80	28.21	27.03	- 4.37
	100	37.84	37.62	- 0.58
	120	46.33	47.19	+ 1.81
2800 rpm	40	19.96	16.00	- 24.74
	60	23.57	22.97	- 2.61
	80	31.26	27.89	- 12.08
	100	39.08	40.47	+ 3.45
	120	48.12	50.41	+ 4.55

Area under the pressure curve results:

	Load (Nm)	Experimental area (bar*deg)	Area after Lambert W function (bar*deg)	% Difference
2000 rpm	20	1220.30	1261.73	+ 3.28
	40	1750.34	1759.88	+ 0.54
	60	2261.20	2353.37	+ 3.92
	80	2786.74	2801.03	+ 0.51
	100	3316.47	3412.11	+ 2.80
	120	3787.70	3759.78	- 0.74
2400 rpm	40	1010.60	1098.79	+ 8.03
	60	1447.88	1377.57	- 5.10
	80	2029.10	1971.18	- 2.94
	100	2670.53	2592.90	- 2.99
	120	3238.00	3177.81	- 1.89
2800 rpm	40	1434.97	1223.22	- 17.23
	60	1682.46	1642.24	- 2.45
	80	2212.54	2032.06	- 8.88
	100	2754.27	2818.42	+ 2.28
	120	3371.55	3478.82	+ 3.08

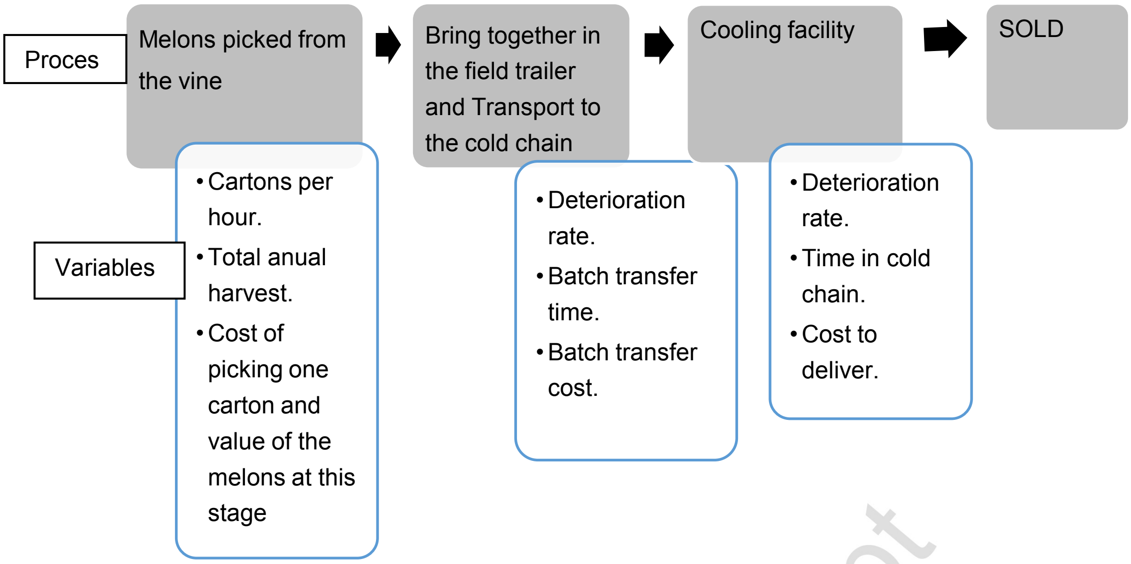

Figure 1: Melon supply chain presented by (Blackburn & Scudder, 2009) for Economic Order Quantity Problem with perishable inventory.

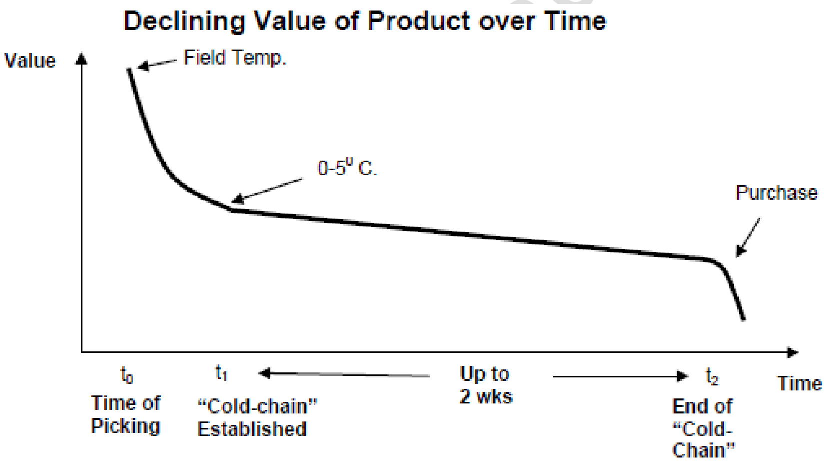

Figure 2: Reduction of the value of the product over time. Reproduced from *(Blackburn & Scudder, 2009)*.

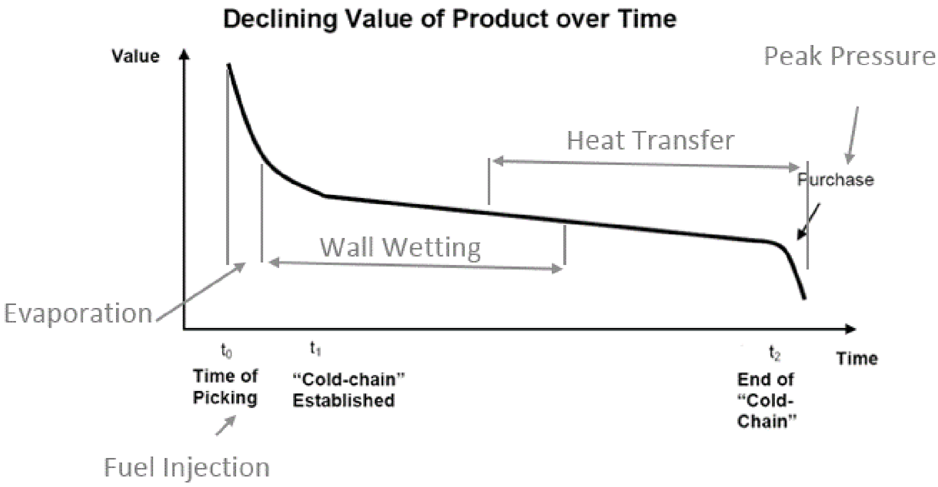

Figure 3: Analogy between economic order quantity and fuel injection event.

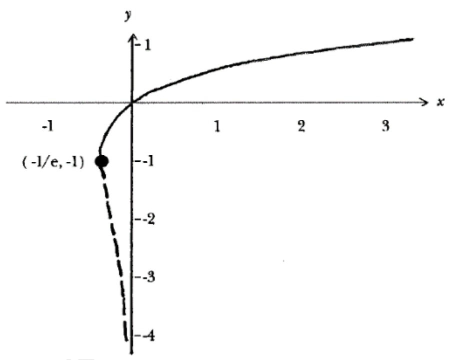

Figure 4*:* Plot of the Lambert W function. The solid line shows W0[z] while the dashed line shows W-1[z]. (Stewart, 2005).

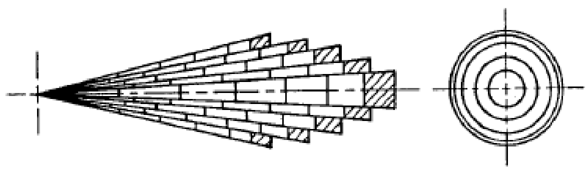

Figure 5: Divided package of spray *(Hiroyasu, et al., 1993)*.

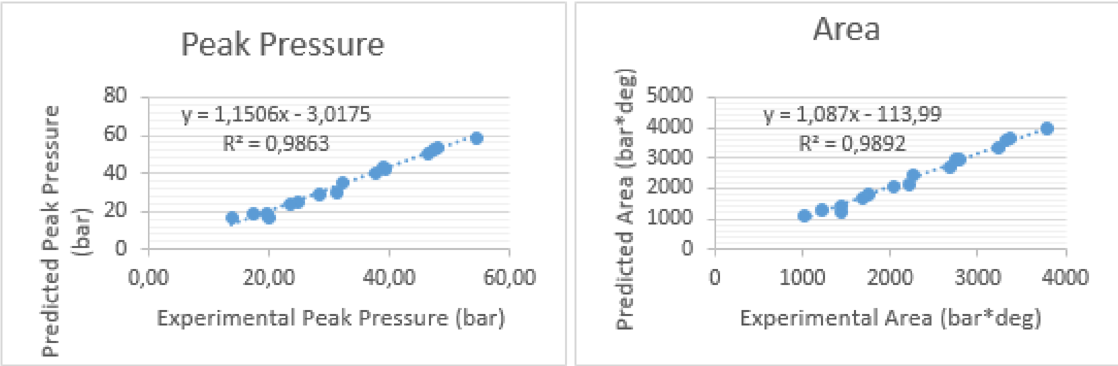

Figure 6: Experimental and Predicted peak cylinder pressure and indicated mean effecting pressure for validation purpose (2000, 2400 and 2800 rpm engine speed and 20, 40, 60. 80, 100 and 120 Nm load conditions).

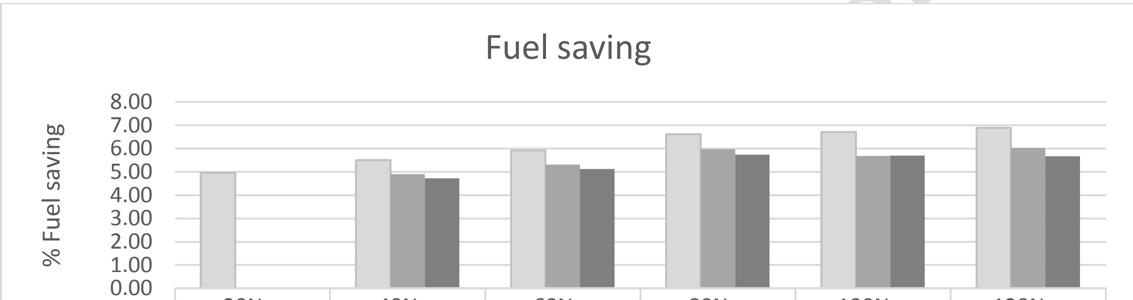

	20Nm	40Nm	60Nm	80Nm	100Nm	120Nm
2000 rpm	4.95	5.50	5.92	6.62	6.71	6.89
2400 rpm		4.91	5.32	5.96	5.68	6.03
2800 rpm		4.72	5.11	5.74	5.70	5.66

Figure 7: Fuel saving at each load and engine speed condition.

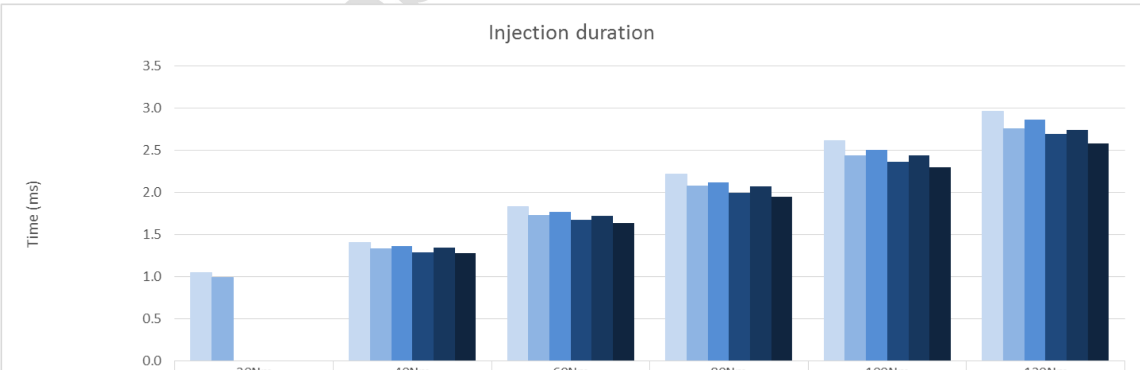

	20Nm	40Nm	60Nm	80Nm	100Nm	120Nm
2000 rpm	1.0474	1.4085	1.8364	2.2206	2.6126	2.9642
Optimized 2000 rpm	0.99555	1.3311	1.7278	2.0737	2.4374	2.7599
2400 rpm		1.3616	1.7757	2.1249	2.5066	2.8657
Optimized 2400 rpm		1.2948	1.6813	1.9982	2.3642	2.6929
2800 rpm		1.3465	1.7286	2.0740	2.4373	2.7415
Optimized 2800 rpm		1.2829	1.6401	1.9551	2.2984	2.5862

Figure 8: Optimized values for injection duration.

Table 1: Analogy between variables.

Economic Order Quantity (melons)	From fuel injector to cylinder pressure
Picking melons: T_0 → initial time P → cartons per hour v → value of the melons at picking	**Injection Event:** T_0 → initial time P → Injected fuel mass quantity per cycle (kg/cycle) v → Heating value at T_0 (J/kg)
Bring together in the field trailer and to another vehicle: α → Deterioration rate t_r → Batch transfer time K → Batch transfer cost	**Direct Injecton to the cylinder** α → Deterioration rate during evaporation and wall wetting (kg/s) t_r → Wall wetting duration K → Total cost of evaporation and wall wetting (J)
Cooling facility: β → Deterioration rate t_j → Time in the cold chain	**Heat transfer:** β → Deterioration rate during heat transfer (kg/s) t_j → Heat transfer duration
SOLD: Decision variable → Q cases of melons	**PEAK PRESSURE:** Decision variable → Quantity of fuel not to be injected (to substract from the original fuel mass injected) (kg)

Table 2: GDI test engine technical specifications.

Bore	77 mm
Stroke	85.8 mm
Compression ratio	10.5
Displacement	1598 cc
Rated Power	173 bhp @ 5500 rpm
Rated torque	240 Nm @ 1700-4500 rpm
Maximum fuel injection pressure	120 bar

Table 3: Summary of results regarding fuel saving.

	Load (Nm)	Fuel injected (kg)	Optimized fuel to be injected (kg)	% Fuel saving when EOQ is applied
2000 rpm	20	7.28E-06	6.92E-06	4.95
	40	1.05E-05	9.88E-06	5.50
	60	1.39E-05	1.31E-05	5.92
	80	1.71E-05	1.60E-05	6.62
	100	2.13E-05	1.99E-05	6.71
	120	2.53E-05	2.36E-05	6.89
2400 rpm	40	9.73E-06	9.25E-06	4.91
	60	1.32E-05	1.25E-05	5.32
	80	1.62E-05	1.52E-05	5.96
	100	2.11E-05	1.99E-05	5.68

	120	2.47E-05	2.32E-05	6.03
2800 rpm	40	9.62E-06	9.16E-06	4.72
	60	1.34E-05	1.27E-05	5.11
	80	1.60E-05	1.51E-05	5.74
	100	2.10E-05	1.98E-05	5.70
	120	2.47E-05	2.33E-05	5.66

529 **Table 4:** Air-fuel ratio at each engine condition after applying Lambert W function.

	Load (Nm)	Air-fuel ratio after applying Lambert W function
2000 rpm	20	15.4661
	40	15.5553
	60	15.6242
	80	15.7415
	100	15.7565
	120	15.7883
2400 rpm	40	15.4583
	60	15.5255
	80	15.6324
	100	15.5858
	120	15.6433
2800 rpm	40	15.4287
	60	15.4924
	80	15.5944
	100	15.5887
	120	15.5825

530